Synthetic, Structural, and Kinetic Studies of $[CpRu(CO)_2(\mu_2\text{-}\eta^1(S):\eta^6\text{-DBT})RuCp^*][PF_6]_2$: A Dibenzothiophene Bridge between Two Ruthenium Fragments

Paul A. Vecchi, Arkady Ellern,† and Robert J. Angelici*

Ames Laboratory and Department of Chemistry, Iowa State University, Ames, Iowa 50011-3111

Received March 4, 2005

The complexes $[CpRu(CO)_2(\mu_2\text{-}\eta^1(S):\eta^6\text{-DBT})RuCp']^{2+}$ ($Cp' = \eta^5\text{-}C_5H_5$ (**3**), $\eta^5\text{-}C_5Me_5$ (**4**)) were synthesized and shown by X-ray crystallography to contain a bridging dibenzothiophene ligand that is coordinated to $\{CpRu(CO)_2\}^+$ through the sulfur atom and to $\{Cp'Ru\}^+$ through an arene ring (η^6). Kinetic studies of the displacement of the $[Cp^*Ru(\eta^6\text{-DBT})]^+$ moiety in **4** by $P(OPh)_3$ show that the η^6-coordinated $\{Cp^*Ru\}^+$ group weakens the Ru−S bond, as compared to that in $[CpRu(CO)_2(\eta^1(S)\text{-DBT})]^+$, and greatly increases the rate of DBT dissociation.

Introduction

The removal of sulfur compounds from transportation fuels is important for the elimination of NO_x and SO_x atmospheric pollution.[1] The main process by which sulfur is currently removed from petroleum feedstocks is through an industrial catalytic process known as hydrodesulfurization (HDS).[2] One of the most difficult classes of sulfur compounds to process using HDS is the dibenzothiophenes (Figure 1), which are found mainly in diesel fuel. To reduce the amount of pollution from diesel fuel combustion, the United States has mandated a reduction in sulfur levels from the current average of 500 ppm to 15 ppm starting in 2006.[1a,3] Europe has a similar plan in place with a goal of 2008.[3a,4] The removal of dibenzothiophenes from diesel fuels is necessary in order to meet these low sulfur requirements.

Various new approaches to the removal of dibenzothiophenes (DBTh) from diesel feedstocks take advantage of the ability of DBTh to bind to transition metals in their complexes.[5] The two most common binding modes of dibenzothiophenes in transition-metal compounds are η^1(S), where coordination occurs through the sulfur atom, and η^6, where binding occurs to one (or both) of the dibenzothiophene rings. It has been reported that η^6 coordination affects reactions that occur at the sulfur of DBT. Sweigart and co-workers demonstrated that η^6 coordination of dibenzothiophene to a cationic $\{Mn(CO)_3\}^+$ fragment activates the C−S bond to cleavage by $Pt(PPh_3)_2$, a process that is proposed to occur after formation of a short-lived η^1(S) intermediate.[6,7] An earlier study in this group showed that η^6 coordination of benzothiophene (Figure 1) to a neutral $\{Cr(CO)_3\}$ fragment causes the benzothiophene to favor η^2-olefin binding to $\{CpRe(CO)_2\}$ over η^1(S) coordination.[8] This was attributed to a decrease in the electron-donating ability of the sulfur atom caused by the electron-withdrawing $Cr(CO)_3$ fragment; without the η^6-$\{Cr(CO)_3\}$ group, the $CpRe(CO)_2BT$ complex exists as an equilibrium mixture of η^2 and η^1(S) complexes. In the present study, we examine the ability of an η^6 coordinated $\{Cp'Ru\}^+$ group on DBT to influence its binding through sulfur to $\{CpRu(CO)_2\}^+$. As part of this investigation, we characterize complexes in which DBT is both η^6 and η^1(S) coordinated to cyclopentadienyl ruthenium units. Kinetic studies of the cleavage of the Ru−S bond in $[CpRu(CO)_2(\mu_2\text{-}\eta^1(S):\eta^6\text{-DBT})RuCp^*][PF_6]_2$ show that the η^6 coordinated $\{Cp^*Ru\}^+$ unit weakens this Ru−S bond.

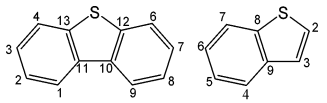

Figure 1. Numbering schemes for dibenzothiophene (DBT) and benzothiophene (BT).

* To whom correspondence should be addressed. Fax: 515-294-0105. E-mail: angelici@iastate.edu.
† Molecular Structure Laboratory, Iowa State University, Ames, IA 50011-3111.

(1) (a) Whitehurst, D. D.; Isoda, T.; Mochida, I. *Adv. Catal.* **1998**, *42*, 345. (b) Gates, B. C.; Topsøe, H. *Polyhedron* **1997**, *16*, 3213. (c) Angelici, R. J. In *Encyclopedia of Inorganic Chemistry*; King, R. B., Ed.; Wiley: New York, 1994; p 1433. (d) Ho, T. C. *Catal. Rev.* **1988**, *30*, 117.
(2) Topsøe, H.; Clausen, B. S.; Massoth, F. E. *Hydrotreating Catalysis: Science and Technology*; Springer-Verlag: Berlin, 1996.
(3) (a) Ho, T. C. *Catal. Today* **2004**, *98*, 3. (b) Song, C. *Catal. Today* **2003**, *86*, 211 and references therein. (c) Borushko, M. *Fed. Regist.* **2001**, *66*, 5001.
(4) Torres-Nieto, J.; Arevalo, A.; Garcia-Gutierrez, P.; Acosta-Ramirez, A.; Garcia, J. J. *Organometallics* **2004**, *23*, 4534.
(5) Sánchez-Delgado, R. A. *Organometallic Modeling of the Hydrodesulfurization and Hydrodenitrogenation Reactions*; Kluwer Academic: Dordrecht, The Netherlands, 2002.
(6) Oh, M.; Yu, K.; Li, H.; Watson, E. J.; Carpenter, G. B.; Sweigart, D. A. *Adv. Synth. Catal.* **2003**, *345*, 1053.
(7) (a) Yu, K.; Li, H.; Watson, E. J.; Virkaitis, K. L.; Carpenter, G. B.; Sweigart, D. A. *Organometallics* **2001**, *20*, 3550. (b) Li, H.; Carpenter, G. B.; Sweigart, D. A. *Organometallics* **2000**, *19*, 1823. (c) Dullaghan, C. A.; Zhang, X.; Greene, D. L.; Carpenter, G. B.; Sweigart, D. A.; Camiletti, C.; Rajaseelan, E. *Organometallics* **1998**, *17*, 3316.
(8) Rudd, J. A., II.; Angelici, R. J. *Inorg. Chim. Acta* **1995**, *240*, 393.

10.1021/om050158y CCC: $30.25
Publication on Web 06/11/2005

Experimental Section

General Procedures. All reactions were performed under an atmosphere of dry argon in reagent grade solvents using standard Schlenk techniques. Hexanes, methylene chloride (CH_2Cl_2), and diethyl ether (Et_2O) were purified on alumina using a Solv-Tek solvent purification system similar to that described by Grubbs and co-workers.[9] Nitromethane (CH_3NO_2, 96+%) and deuterated nitromethane (CD_3NO_2), both purchased from Aldrich, were deoxygenated by three freeze−pump−thaw cycles and stored under argon until use. Acetone was stirred with calcium chloride overnight, distilled, subjected to three freeze−pump−thaw cycles, and stored under argon, while 1,2-dichloroethane (DCE) was stirred overnight with P_2O_5 before being distilled, deoxygenated, and stored under argon. Neutral alumina (Brockman, activity I) was deoxygenated under vacuum for 24 h, deactivated with 7.5% w/w argon-saturated water (Ultrapure), and stored under argon until use. Dibenzothiophene (DBT) was purchased from Aldrich and sublimed before use. Solid $AgPF_6$ (99.99+%) and $AgBF_4$ (99.99+%) were purchased from Aldrich and used without further purification. The complexes $[CpRu(NCMe)_3][PF_6]$,[10] $CpRu(CO)_2Cl$,[11] $[CpRu(CO)_2(\eta^1(S)\text{-DBT})][BF_4]$,[12] $[Cp^*Ru(NCMe)_3][PF_6]$,[13] and $[Cp^*Ru(\mu_3\text{-Cl})]_4$[14] were all prepared according to published literature methods. Filtrations were performed through a plug of filter paper, Celite, and cotton that was prepared from a cut 1 mL syringe, and the solutions were transferred via thin-wall Teflon tubing (Alpha Wire Corp.).

Solution ^1H and $^{13}C\{^1H\}$ NMR spectra were recorded on a Bruker DRX-400 spectrometer using CD_3NO_2 as the solvent, internal lock, and reference (δ 4.33 (^1H), 62.8 (^{13}C)). Solution infrared spectra of the compounds in CH_3NO_2 were recorded on a Nicolet-560 spectrometer using NaCl cells with 0.1 mm spacers. Elemental analyses were performed on a Perkin-Elmer 2400 Series II CHNS/O analyzer.

$[CpRu(\eta^6\text{-DBT})][PF_6]$ (1). This complex was prepared in a manner similar to that reported previously.[15] To solid $[CpRu(NCMe)_3][PF_6]$ (100 mg, 0.230 mmol) and DBT (63.6 mg, 0.345 mmol) was added 20 mL of DCE, and the solution was gently refluxed for 15 h. The solution was cooled to room temperature and filtered into diethyl ether to precipitate the product. The tan solid was isolated by filtration and washed with both diethyl ether and hexanes to remove any excess DBT. Reaction yields were greater than 95% before workup, as described next. The crude solid product was dissolved in 5 mL of acetone and filtered onto a short column of alumina packed in hexanes. The product was eluted with a 1:1 acetone−CH_2Cl_2 solution, leaving an unidentified tan impurity on the column. The solvents were removed from the eluant under vacuum; the remaining solid was redissolved in CH_2Cl_2, and the resulting solution was filtered into cold diethyl ether to precipitate the pure product. Removal of the solvent by filtration yielded 89.0 mg (0.180 mmol) of $[CpRu(\eta^6\text{-DBT})][PF_6]$ (**1**) as a white solid in 78% overall yield. This method of purification was superior to recrystallization from benzene, which was used previously.[15] ^1H NMR (400 MHz, CD_3NO_2): δ 8.27 (d, $^3J(H,H) = 7.6$ Hz, 1H), 7.93 (d, $^3J(H,H) = 7.6$ Hz, 1H), 7.71 (t, $^3J(H,H) = 7.6$ Hz, 1H), 7.62 (t, $^3J(H,H) = 7.6$ Hz, 1H), 7.33 (d, $^3J(H,H) = 5.6$ Hz, 1H), 7.21 (d, $^3J(H,H) = 5.6$ Hz, 1H), 6.38−6.27 (d-of-t, $^3J(H,H) = 5.6$ Hz, 2H), DBT; 5.12 (s, 5H), Cp. $^{13}C\{^1H\}$ NMR (100.6 MHz, CD_3NO_2): δ 142.01, 133.38, 131.83, 127.53, 124.93, 124.90, 111.19, 101.46, 85.07, 84.65, 81.82, 79.67 (DBT); 82.73 (Cp).

$[Cp^*Ru(\eta^6\text{-DBT})][PF_6]$ (2). Method A. To solid $[Cp^*Ru(NCMe)_3][PF_6]$ (200 mg, 0.396 mmol) and DBT (110 mg, 0.597 mmol) was added 25 mL of DCE, and the solution was gently refluxed for 15 h. Evaporation of the solvent yielded a tan residue, which was washed with both diethyl ether and hexanes to remove any excess DBT. Reaction yields were nearly quantitative before workup, which was performed in the manner described above for **1**. After isolation, 178 mg (0.315 mmol) of $[Cp^*Ru(\eta^6\text{-DBT})][PF_6]$ (**2**) was obtained as a white, air-stable solid (79% yield). ^1H NMR (400 MHz, CD_3NO_2): δ 8.15 (d, $^3J(H,H) = 7.6$ Hz, 1H), 7.96 (d, $^3J(H,H) = 7.6$ Hz, 1H), 7.71−7.61 (m, 2H), 6.79 (d, $^3J(H,H) = 5.2$ Hz, 1H), 6.64 (d, $^3J(H,H) = 5.2$ Hz, 1H), 6.05−5.99 (m, 2H), DBT; 1.61 (s, 15H), Cp*. $^{13}C\{^1H\}$ NMR (100.6 MHz, CD_3NO_2): δ 141.60, 132.51, 131.34, 127.60, 124.89, 124.78, 109.78, 100.32, 87.49, 87.28, 83.38, 81.19 (DBT); 96.92, 9.45 (Cp*). Anal. Calcd for $C_{22}H_{23}F_6PRuS$: C, 46.72; H, 4.10. Found: C, 46.66; H, 4.31.

Method B. To a 50 mL Schlenk flask containing freshly prepared $[Cp^*Ru(\mu_3\text{-Cl})]_4$ (180 mg, 0.166 mmol), DBT (183 mg, 0.993 mmol), and $AgPF_6$ (172 mg, 0.680 mmol) was added 25 mL of CH_2Cl_2. The reaction solution was stirred at room temperature for 2 h, during which time the solution color changed from dark orange to light yellow with formation of a AgCl precipitate. The reaction solution was then filtered into cold diethyl ether to give **2**, which was isolated and purified as described above. Using this method, 325 mg (0.575 mmol) of white $[Cp^*Ru(\eta^6\text{-DBT})]PF_6$ (**2**) was obtained (87% yield).

Synthesis of $[CpRu(CO)_2(\mu_2\text{-}\eta^1(S)\text{:}\eta^6\text{-DBT})RuCp][PF_6]_2$ (3). A flask containing solid $CpRu(CO)_2Cl$ (50.0 mg, 0.194 mmol), $[CpRu(\eta^6\text{-DBT})][PF_6]$ (95.0 mg, 0.192 mmol), and $AgPF_6$ (52.0 mg, 0.206 mmol) was placed in an ice bath, and 5 mL of cold CH_2Cl_2 was added. The solution was stirred at 0 °C for 1 h, during which time the yellow solution color lightened and a light-colored precipitate formed. The reaction mixture was allowed to settle for a few minutes before the solution was removed by filtration. The remaining solid was extracted with 1 mL of CH_3NO_2 and filtered into cold diethyl ether, precipitating the pale yellow product. This solid was isolated by filtration, washed with a small amount of cold CH_2Cl_2 (<1 mL) and dried under vacuum to obtain 103 mg (0.119 mmol) of $[CpRu(CO)_2(\mu_2\text{-}\eta^1(S)\text{:}\eta^6\text{-DBT})RuCp][PF_6]_2$ (**3**) as a moderately air-stable powder (62% yield). Compound **3** is insoluble in diethyl ether and hexanes and minimally soluble in CH_2Cl_2. Although it is soluble in CH_3NO_2 and acetone, compound **3** decomposes in solution at room temperature and must be kept cold for NMR characterization. ^1H NMR (400 MHz, CD_3NO_2, 273 K): δ 8.29 (d, $^3J(H,H) = 7.6$ Hz, 1H), 8.00 (d, $^3J(H,H) = 7.6$ Hz, 1H), 7.90−7.80 (m, 2H), 7.45−7.42 (m, 1H), 7.25−7.22 (m, 1H), 6.55−6.53 (m, 2H), DBT; 5.90 (s, 5H), 5.35 (s, 5H) Cp. $^{13}C\{^1H\}$ NMR (100.6 MHz, CD_3NO_2, 273 K): δ 194.14, 193.80 (CO); 141.60, 134.11, 133.81, 131.93, 127.47, 126.24, 110.07, 101.82, 86.89, 86.65, 84.31, 81.50 (DBT); 91.35, 84.81 (Cp). IR (CH_3NO_2): ν(CO) (cm^{-1}) 2082 (s), 2039 (s). Anal. Calcd for $C_{24}H_{18}F_{12}O_2P_2Ru_2S$: C, 33.42; H, 2.10; S, 3.72. Found: C, 33.13; H, 1.64; S, 3.88.

$[CpRu(CO)_2(\mu_2\text{-}\eta^1(S)\text{:}\eta^6\text{-DBT})RuCp^*][X]_2$ (X = PF_6^- (4a), BF_4^- (4b)). Method A. A flask containing solid $CpRu(CO)_2Cl$ (150 mg, 0.582 mmol), $[Cp^*Ru(\eta^6\text{-DBT})]PF_6$ (326 mg, 0.576 mmol), and $AgPF_6$ (150 mg, 0.593 mmol) was placed in an ice bath, and 15 mL of cold CH_2Cl_2 was added. The solution was stirred at 0 °C for 1 h, during which time the solution color lightened and a precipitate formed. The solution was then filtered into cold diethyl ether, resulting in precipitation of a pale yellow product. The remaining solid in the reaction vessel was dissolved in 2 mL of CH_3NO_2, and this solution was also filtered into the cold diethyl ether to precipitate the rest of the product. The pale yellow solid was isolated by filtration, followed by drying under vacuum to give 441 mg (0.473 mmol)

(9) Pangborn, A. B.; Giardello, M. A.; Grubbs, R. H.; Rosen, R. K.; Timmers, F. J. *Organometallics* **1996**, *15*, 1518.
(10) Gill, T. P.; Mann, K. R. *Organometallics* **1982**, *1*, 485.
(11) Eisenstadt, A.; Tannenbaum, R.; Efraty, A. *J. Organomet. Chem.* **1981**, *221*, 317.
(12) Benson, J. W.; Angelici, R. J. *Organometallics* **1993**, *12*, 680.
(13) Schrenk, J. L.; McNair, A. M.; McCormick, F. B.; Mann, K. R. *Inorg. Chem.* **1986**, *25*, 3501.
(14) (a) Fagan, P. J.; Ward, M. D. Calabrese, J. C. *J. Am. Chem. Soc.* **1989**, *111*, 1698. (b) Fagan, P. J.; Mahoney, W. S.; Calabrese, J. C.; Williams, I. D. *Organometallics* **1990**, *9*, 1843.
(15) Wang, C.-M. J.; Angelici, R. J. *Organometallics* **1990**, *9*, 1770.

of $[CpRu(CO)_2(\mu_2\text{-}\eta^1(S):\eta^6\text{-DBT})RuCp^*][PF_6]_2$ (**4a**) as a moderately air-stable solid (82% yield). If impurities are present, they can be removed by washing with a small amount (<1 mL) of cold CH_2Cl_2. ^1H NMR (400 MHz, CD_3NO_2, 273 K): δ 8.25−8.22 (m, 1H), 8.08−8.05 (m, 1H), 7.89−7.86 (m, 2H), 6.97 (d, $^3J(H,H) = 5.6$ Hz, 1H), 6.83 (d, $^3J(H,H) = 5.6$ Hz, 1H), 6.32−6.26 (m, 2H), DBT; 5.88 (s, 5H), Cp; 1.68 (s, 15H), Cp*. $^{13}C\{^1H\}$ NMR (100.6 MHz, CD_3NO_2, 273 K): δ 194.15, 193.77 (CO); 141.23, 133.43, 133.21, 132.26, 127.55, 126.06, 108.41, 100.09, 89.04, 88.75, 85.08, 83.03 (DBT); 91.34 (Cp); 99.66, 9.60 (Cp*). IR (CH_3NO_2): ν(CO) (cm^{-1}) 2081 (s), 2038 (s). Anal. Calcd for $C_{29}H_{28}F_{12}O_2P_2Ru_2S$: C, 37.35; H, 3.03; S, 3.44. Found: C, 36.89; H, 2.89; S, 3.31.

Method B. A reaction vessel containing solid $[CpRu(CO)_2(\eta^1(S)\text{-DBT})][BF_4]$ (50.0 mg, 0.101 mmol), freshly prepared $[Cp^*Ru(\mu_3\text{-Cl})]_4$ (27.5 mg, 0.0253 mmol), and $AgBF_4$ (20.0 mg, 0.103 mmol) was placed in an ice bath, and 2 mL of cold CH_3NO_2 was added. The mixture was stirred for 1 h, during which time the dark orange solution changed to yellow, and a precipitate was observed. The solution was then filtered into another flask containing cold diethyl ether to precipitate the product. The solid was isolated by filtration, washed with 1 mL of cold CH_2Cl_2, and dried under vacuum to yield 52.0 mg (0.0637 mmol) of $[CpRu(CO)_2(\mu_2\text{-}\eta^1(S):\eta^6\text{-DBT})RuCp^*][BF_4]_2$ (**4b**) as a light yellow powder (63% yield). The solution ^1H and $^{13}C\{^1H\}$ NMR spectra in CD_3NO_2 were nearly identical with those reported above for **4a**.

X-ray Structural Determination of $[CpRu(CO)_2(\mu_2\text{-}\eta^1(S):\eta^6\text{-DBT})RuCp^*][PF_6]_2$ (4a). A yellow single crystal of **4a** suitable for an X-ray diffraction study was obtained by layering a cold acetone solution of the complex with Et_2O under argon and storing at −25 °C for 1 week. The crystal was selected from the mother liquor under ambient conditions and quickly coated in premixed epoxy glue. The covered crystal was mounted onto the end of a glass fiber, placed under a stream of cold nitrogen, and centered in the X-ray beam using a video camera. Crystal evaluation and data collection were performed at 173 K on a Bruker CCD-1000 diffractometer with Mo Kα ($\lambda = 0.710\ 73$ Å) radiation and a collector-to-crystal distance of 5.03 cm. Cell constants were determined from a list of reflections found by an automated search routine. Data were collected using the full-sphere routine and were corrected for Lorentz and polarization effects. The absorption correction was based on fitting a function to the empirical transmission surface, as sampled by multiple equivalent measurements using SADABS software.[16] Positions of the heavy atoms were found by the Patterson method. The remaining atoms were located in an alternating series of least-squares cycles and difference Fourier maps. All non-hydrogen atoms were refined using a full-matrix anisotropic approximation. Hydrogen atoms were placed in the structure factor calculations at idealized positions and refined using a riding model. Other crystallographic data are given in Table 1.

Kinetic Studies. Solutions of $[CpRu(CO)_2(\mu_2\text{-}\eta^1(S):\eta^6\text{-DBT})RuCp^*][PF_6]_2$ (**4a**) and liquid $P(OPh)_3$ were prepared for kinetic studies according to the following procedure: a 0.010 mmol sample of the complex was added to an NMR tube, and the tube was evacuated and flushed with argon. To the NMR tube was first added CD_3NO_2, followed immediately by $P(OPh)_3$, such that the total volume of the reaction solution was always 0.50 mL. The tube was capped tightly with a septum, shaken, and immediately placed into the probe of a Bruker DRX-400 NMR spectrometer thermostated at 25.0 ± 0.1 °C. The spectrometer was preprogrammed to acquire spectra at specific time intervals. Three independent experiments were carried out for five different concentrations of $P(OPh)_3$. The products formed during the course of the reactions were $[CpRu(CO)_2(P(OPh)_3)]^+$ [17] and $[Cp^*Ru(\eta^6\text{-DBT})]^+$, which were identified by their NMR spectra. Concentrations of reactants and products were determined by integration of the Cp and Cp* signals in the ^1H NMR spectrum.

Table 1. Crystal Data and Structure Refinement Details for $[CpRu(CO)_2\{\mu_2\text{-}\eta^1(S):\eta^6\text{-DBT}\}RuCp^*][PF_6]_2\cdot 2(CH_3)_2CO$ (4a)

empirical formula	$C_{29}H_{28}F_{12}O_2P_2Ru_2S\cdot 2C_3H_6O$
formula wt	1048.81
temp (K)	173(2)
wavelength (Å)	0.710 73
cryst syst	monoclinic
space group	$P2_1/c$
unit cell dimens	
a (Å)	14.475(3)
b (Å)	13.038(2)
c (Å)	21.687(3)
α (deg)	90.000
β (deg)	95.772(5)
γ (deg)	90.000
V (Å^3)	4072.0(12)
Z	4
density (calcd)	1.711 Mg/m^3
abs coeff	0.963 mm^{-1}
F(000)	2096
cryst size	0.30 × 0.30 × 0.23 mm^3
θ range for data collection	1.82−28.19°
index ranges	$-18 \le h \le 13$, $-15 \le k \le 15$, $-28 \le l \le 8$
no. of rflns collected	13 059
no. of indep rflns	6448 (R(int) = 0.0358)
completeness to θ	96.5% (θ = 22.00°)
abs cor	semiempirical from equivalents
max and min transmn	1.00 and 0.71
refinement method	full-matrix least squares on F^2
no. of data/restraints/params	6448/0/505
goodness of fit on F^2	1.042
final R^a indices ($I > 2\sigma(I)$)	R1 = 0.0325, wR2 = 0.0869
R^a indices (all data)	R1 = 0.0376, wR2 = 0.0900
largest diff peak and hole	0.698 and −0.450 e Å^{-3}

[a] $R1 = \sum||F_o| - |F_c||/\sum|F_o|$ and $wR2 = \{\sum[w(F_o^2 - F_c^2)^2]/\sum[w(F_o^2)^2]\}^{1/2}$.

Results and Discussion

Synthesis and Characterization of $[CpRu(CO)_2(\mu_2\text{-}\eta^1(S):\eta^6\text{-DBT})RuCp'][PF_6]_2$ (Cp′ = Cp (3), Cp* (4a)). The precursor complexes $[Cp'Ru(\eta^6\text{-DBT})][PF_6]$ (Cp′ = Cp (**1**), Cp* (**2**)) are prepared in high yields by reactions of $[Cp'Ru(NCMe)_3][PF_6]$ with DBT in DCE in a manner similar to that described previously for $[CpRu(\eta^6\text{-DBT})][PF_6]$.[15] Both **1** and **2** are soluble in acetone, methylene chloride, and nitromethane and insoluble in hexanes and diethyl ether. Compound **2** may also be prepared by the reaction of freshly prepared $[Cp^*Ru(\mu_3\text{-Cl})]_4$ with $AgPF_6$ and DBT in CH_2Cl_2 at room temperature. This method is preferred because the starting material $[Cp^*Ru(\mu_3\text{-Cl})]_4$ is more readily prepared than $[Cp^*Ru(NCMe)_3][PF_6]$, and the reaction to form $[Cp^*Ru(\eta^6\text{-DBT})][PF_6]$ is complete within 2 h at room temperature as opposed to refluxing in DCE for longer periods of time. It also allows for direct incorporation of different anions into **2** by appropriate choice of the silver salt. The solution NMR spectra of **1** and **2** exhibit ^1H and ^{13}C signals for the uncoordinated ring of DBT with chemical shifts that are similar to those of free DBT (^1H NMR (400 MHz, CD_3NO_2) δ 8.27−8.24 (m, 2H), 7.95−7.94 (m, 2H), 7.55−7.50 (m, 4H); $^{13}C\{^1H\}$ NMR (100.6 MHz, CD_3NO_2) δ 140.65, 136.85, 128.36, 125.99, 124.15, 123.04). There are also signals that are

(16) Blessing, R. H. *Acta Crystallogr.* **1995**, *A51*, 33.

(17) Nakazawa, H.; Kawamura, K.; Kubo, K.; Miyoshi, K. *Organometallics* **1999**, *18*, 2961.

upfield by 0.9−1.5 and 28−45 ppm in the ^{1}H and ^{13}C-{^{1}H} NMR spectra, respectively, for the DBT ring that is η^6 coordinated to the {Cp′Ru}$^+$ fragment, as reported previously for [CpRu(η^6-DBT)][PF_6].[15]

The compounds [$CpRu(CO)_2(\mu_2$-$\eta^1(S)$:η^6-DBT)RuCp′]-[PF_6]$_2$ (Cp′ = Cp (**3**), Cp* (**4a**)), with μ_2-$\eta^1(S)$:η^6 bridging DBT ligands, are prepared by reactions of $CpRu(CO)_2Cl$ with $AgPF_6$ and the appropriate [Cp′Ru(η^6-DBT)][PF_6] in cold CH_2Cl_2, as shown in eq 1.

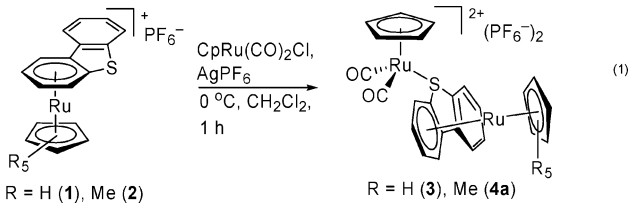

Alternatively, [$CpRu(CO)_2(\mu_2$-$\eta^1(S)$:η^6-DBT)RuCp*]-[BF_4]$_2$ (**4b**) was prepared by reaction of [$CpRu(CO)_2(\eta^1$-(S)-DBT)][BF_4] with [Cp*Ru(μ_3-Cl)]$_4$ and $AgBF_4$ in cold CH_2Cl_2. Compounds **3** and **4** are moderately stable as solids but undergo some decomposition in solution by dissociation of the [Cp′Ru(η^6-DBT)]$^+$ unit at room temperature. Therefore, their NMR spectra in CD_3NO_2 solvent were recorded at 273 K, at which temperature both complexes were stable indefinitely. The chemical shifts of the DBT protons in **3** and **4** are shifted slightly (0.02−0.27 ppm) downfield as compared to those of the free [Cp′Ru(η^6-DBT)]$^+$ ligands. Similar small downfield shifts in the proton NMR signals of η^1(S)-coordinated DBT were observed in [$CpFe(CO)_2(\eta^1(S)$-DBT)]$^+$,[18] and [$CpRu(CO_2)(\eta^1(S)$-DBT)]$^+$.[12] Shifts for the hydrogen and carbon atoms of the η^6-coordinated DBT ring in compounds **3** and **4** remain significantly upfield of those in free DBT, as they are in **1** and **2**.

The ^{13}C{^{1}H} NMR spectra for both **3** and **4a** at 273 K show two distinct chemical resonances for the two diastereotopic CO ligands. On the other hand, the benzothiophene complexes [$CpFe(CO)_2(\eta^1(S)$-BT)]$^+$ [18] and [$CpRu(CO)_2(\eta^1(S)$-BT)]$^+$ [12] contain only one carbonyl resonance at room temperature. The occurrence of only one CO signal in these compounds is attributed to a dynamic process in which there is inversion at the sulfur atom coupled with rapid rotation around the M−S bond. Only upon cooling CD_2Cl_2 solutions of [$CpFe(CO)_2(\eta^1$-(S)-BT)]$^+$ and [$CpRu(CO)_2(\eta^1(S)$-BT)]$^+$ to 170 and 198 K, respectively, was it possible to observe both diastereotopic carbonyl signals by NMR and to calculate the free energies of activation ($\Delta G^‡$) for sulfur inversion: $\Delta G^‡$ = 39 kJ/mol at 190 K (T_c) for [$CpFe(CO)_2(\eta^1(S)$-BT)]$^+$,[18] and $\Delta G^‡$ = 43 kJ/mol at 205 K (T_c) for [$CpRu(CO)_2(\eta^1(S)$-BT)]$^+$.[12] The observation of two CO signals for **3** and **4a** indicates that the inversion at the sulfur must be much slower than in [$CpFe(CO)_2(\eta^1(S)$-BT)]$^+$ and [$CpRu(CO)_2(\eta^1(S)$-BT)]$^+$, due to a higher inversion barrier. Because of the instabilities of **3** and **4a**, it was not possible to heat their solutions for the purpose of observing coalescence of the carbonyl signals.

Infrared spectra of **3** and **4a** in CH_3NO_2 show ν(CO) absorptions (2082, 2038 cm^{-1} and 2081, 2038 cm^{-1}, respectively) that are 28−39 cm^{-1} higher in energy than those observed for the neutral starting material $CpRu(CO)_2Cl$ (2053, 1999 cm^{-1} in CH_3NO_2). These values are 4−5 cm^{-1} higher than those for [$CpRu(CO)_2(\eta^1(S)$-DBT)]-[BF_4] in CH_3NO_2 (2077, 2033 cm^{-1}), which indicates that the η^6-coordinated {Cp′Ru}$^+$ group reduces the electron-donor ability of the DBT ligand to the {$CpRu(CO)_2$}$^+$ unit.

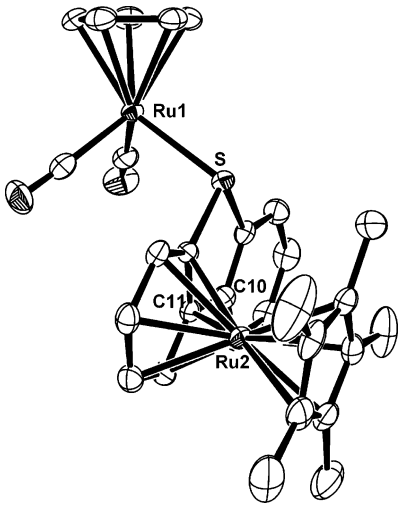

Figure 2. Thermal ellipsoid drawing (ORTEP) of the cation in [$CpRu(CO)_2(\mu_2$-$\eta^1(S)$:η^6-DBT)RuCp*][PF_6]$_2$·2(CH_3)$_2$CO (**4a**·2(CH_3)$_2$CO). Ellipsoids are shown at the 50% probability level; hydrogen, anion, and solvent atoms are omitted for clarity. The Ru−S bond distance is 2.392(1) Å, and the angle defined by Ru−S−Midpt is 114.5°.

The molecular structure (Figure 2) of the cation in [$CpRu(CO)_2(\mu_2$-$\eta^1(S)$:η^6-DBT)RuCp*][PF_6]$_2$ (**4a**), as determined by an X-ray diffraction study, confirms the μ_2-η^1(S):η^6 binding mode for the DBT ligand. Compound **4a** contains a planar DBT ligand that is bound to {$CpRu(CO)_2$}$^+$ through a pyramidal sulfur atom, which is typical of η^1(S)-bonded thiophenes.[5] The [Cp*Ru(η^6-DBT)]$^+$ unit is oriented away from the Cp ligand, and the {Cp*Ru}$^+$ fragment is on the opposite side of the DBT plane from the {$CpRu(CO)_2$}$^+$. The structure of **4a** provides a reasonable explanation for the observation of separate signals for the CO ligands in the ^{13}C{^{1}H} NMR spectrum (see above). If inversion at the sulfur were to occur, as described above for [$CpRu(CO)_2(\eta^1(S)$-BT)]$^+$, the {Cp*Ru}$^+$ and {$CpRu(CO)_2$}$^+$ units in **4a** would be on the same side of the DBT and sterically repel each other. This would reduce the rate of inversion at the sulfur, which would account for the fact that the two CO ligands in the {$CpRu(CO)_2$}$^+$ unit remain inequivalent on the ^{13}C NMR time scale. The Ru−S distance in **4a** (2.392(1) Å) is essentially the same as the corresponding distances in [$CpRu(CO)_2(\eta^1(S)$-DBT)]$^+$ (2.398(2) Å)[19] and [Cp*Ru$(CO)_2(\eta^1(S)$-DBT)]$^+$ (2.394(1) Å).[6a] The tilt angle in **4a**, which is the angle defined by Ru−S-Midpt (where Midpt is the midpoint between the C10 and C11 bond) is 114.5°, which is smaller than the values found for [$CpRu(CO)_2(\eta^1(S)$-DBT)]$^+$ (119.3°),[19] [Cp*Ru$(CO)_2(\eta^1(S)$-DBT)]$^+$ (121.0°),[20a] and [$CpFe(CO)_2$-

(18) Goodrich, J. D.; Nickias, P. N.; Selegue, J. P. *Inorg. Chem.* **1987**, *26*, 3426.

(19) McKinley, S. G.; Vecchi, P. A.; Ellern, A.; Angelici, R. J. *Dalton* **2004**, 788.

(20) (a) Vecchi, P. A.; Ellern, A.; Angelici, R. J. *J. Am. Chem. Soc.* **2003**, *125*, 2064. (b) Vecchi, P. A.; Ellern, A.; Angelici, R. J. *Organometallics* **2005**, *24*, 2168.

Table 2. Rate Constants, k_{obs} (s^{-1}), for Reactions (Eq 2) of 0.020 M $[CpRu(CO)_2(\mu_2\text{-}\eta^1(S)\text{:}\eta^6\text{-DBT})RuCp^*][PF_6]_2$ with $P(OPh)_3$ at 25.0 °C in CD_3NO_2

$[P(OPh)_3]$ (M)	10^4k_{obs}	$[P(OPh)_3]$ (M)	10^4k_{obs}
0.20	0.934	0.80	1.12
	0.946		1.14
	0.965		1.15
0.40	0.996	1.00	1.21
	1.00		1.22
	1.01		1.27
0.60	1.10		
	1.11		
	1.12		

$(\eta^1(S)\text{-DBT})]^+$ (119.4°).[18] These angles are probably determined by crystal packing energies.

Kinetic Studies of $[Cp^*Ru(\eta^6\text{-DBT})]^+$ Substitution by $P(OPh)_3$ in 4a. To determine the effect of the η^6-$\{Cp^*Ru\}^+$ fragment on the lability of the Ru−S bond, the substitution (eq 2) of the $[Cp^*Ru(\eta^6\text{-DBT})]^+$ moiety in **4a** by $P(OPh)_3$ was investigated. These studies were

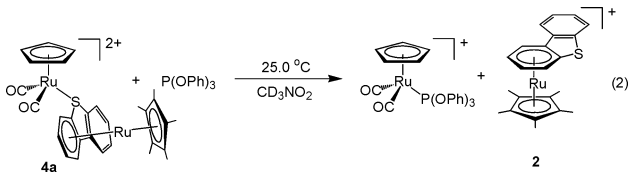

performed under pseudo-first-order conditions with at least a 10-fold excess of the phosphite ligand. First-order plots of the disappearance of **4a** gave rate constants (k_{obs}, Table 2) that follow a two-term rate law (eq 3).

$$k_{obs} = k_1 + k_2[P(OPh)_3] \quad (3)$$

Values of k_1 ($(0.88 \pm 0.03) \times 10^{-4}$ s^{-1}) and k_2 ($(0.34 \pm 0.04) \times 10^{-4}$ M^{-1} s^{-1}) were determined from a graph (Figure 3) of k_{obs} vs $P(OPh)_3$ concentration according to eq 3. The k_1 term presumably corresponds to a pathway in which rate-determining dissociation of the $[Cp^*Ru(\eta^6\text{-DBT})]^+$ from **4a** is followed by rapid addition of $P(OPh)_3$ to give the $[CpRu(CO)_2(P(OPh)_3)]^+$ product. The k_2 term in the rate law most likely corresponds to a dissociative interchange (I_d) mechanism (where the nature of the $[CpRu(CO)_2(\mu_2\text{-}\eta^1(S)\text{:}\eta^6\text{-DBT})RuCp^*][PF_6]\cdot P(OPh)_3$ intermediate is not clear), as was previously suggested by results of kinetic studies of reactions of $[Cp^*Ru(CO)_2(\eta^1(S)\text{-DBTh})][BF_4]$, where DBTh = DBT, 4-MeDBT, 4,6-Me_2DBT, 2,8-Me_2DBT, with PPh_3 and PPh_2Me to give $[Cp^*Ru(CO)_2(PR_3)][BF_4]$.[20b]

In a previous kinetic study[20b] of the reactions (eq 4) of $[CpRu(CO)_2(\eta^1(S)\text{-DBTh})]^+$ complexes (where DBTh = DBT, 4-MeDBT, 4,6-Me_2DBT, and 2,8-Me_2DBT) with $P(OPh)_3$ under the same reaction conditions (CD_3NO_2,

$$[CpRu(CO)_2(\eta^1(S)\text{-DBTh})]^+ + P(OPh)_3 \xrightarrow[CD_3NO_2]{25.0\ °C} [CpRu(CO)_2(P(OPh_3)]^+ + DBTh \quad (4)$$

25.0 °C), the k_1 values decreased in the following order: 4,6-Me_2DBT ($5.18(5) \times 10^{-6}$ s^{-1}) > 4-MeDBT ($4.50(10) \times 10^{-6}$ s^{-1}) > DBT ($4.01(3) \times 10^{-6}$ s^{-1}) > 2,8-Me_2DBT ($1.33(5) \times 10^{-6}$ s^{-1}). In that study, methyl groups in the sterically hindering 4- and 6-positions of DBT were found to increase the kinetic lability of DBT by factors of 1.13 and 1.31, respectively, for 4-MeDBT and 4,6-Me_2-DBT. On the other hand, electron-donating methyl groups in the nonhindering 2,8-positions of DBT reduced the rate by a factor of 0.23. The k_1 value (0.88×10^{-4} s^{-1}) determined in the present study for the dissociation of $[Cp^*Ru(\eta^6\text{-DBT})]^+$ from **4a** shows that η^6 coordination of a $\{Cp^*Ru\}^+$ fragment to the DBT increases the kinetic lability of the DBT ligand by a factor of *22 times*, as compared to the DBT ligand itself. Thus, the $\{Cp^*Ru\}^+$ fragment labilizes the Ru−S bond much more than placing methyl groups in the 4- and 6-positions. The labilizing effect of the $\{Cp^*Ru\}^+$ group is presumably due to the electron-withdrawing ability of the $\{Cp^*Ru\}^+$ group, which reduces the electron-donating ability of the DBT sulfur atom. A steric effect of the $\{Cp^*Ru\}^+$ group is likely to make a smaller contribution to the faster rate for **4a** because of its location on the opposite side of the DBT plane.

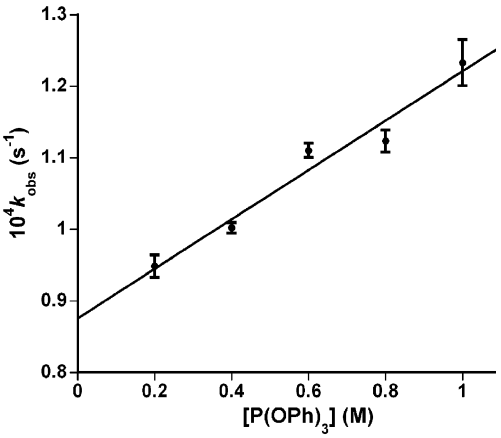

Figure 3. Plot of k_{obs} vs $P(OPh)_3$ concentration (eq 3) for reactions with $[CpRu(CO)_2(\mu_2\text{-}\eta^1(S)\text{:}\eta^6\text{-DBT})RuCp^*][PF_6]_2$ at 25.0 °C in CD_3NO_2.

To determine the relative thermodynamic binding abilities of DBT and $[Cp^*Ru(\eta^6\text{-DBT})]^+$, 0.020 mmol of **4a** was reacted (eq 5) with 0.020 mmol of DBT in 1.0 mL of CD_3NO_2 at 25.0 °C. This resulted in complete

$$\underset{\textbf{4a}}{[CpRu(CO)_2(\mu_2\text{-}\eta^1(S)\text{:}\eta^6\text{-DBT})RuCp^*]^{2+}} + DBT \xrightarrow[25\ °C]{CD_3NO_2} [CpRu(CO)_2(\eta^1(S)\text{-DBT})]^+ + \underset{\textbf{2}}{[Cp^*Ru(\eta^6\text{-DBT})]^+} \quad (5)$$

displacement of the $[Cp^*Ru(\eta^6\text{-DBT})]^+$ group by DBT within 8 h to form only $[CpRu(CO)_2(\eta^1(S)\text{-DBT})]^+$ and $[Cp^*Ru(\eta^6\text{-DBT})]^+$. When the products in eq 5, 0.020 mmol of $[CpRu(CO)_2(\eta^1(S)\text{-DBT})]^+$ and 0.20 mmol of $[Cp^*Ru(\eta^6\text{-DBT})]^+$, were reacted in 1.0 mL of CD_3NO_2 at 25.0 °C, there was no reaction after 1 day. Thus, the η^6 coordination of $\{Cp^*Ru\}^+$ to DBT also substantially reduces the *thermodynamic* binding ability of DBT to $\{CpRu(CO)_2\}^+$.

Conclusions

Dibenzothiophene forms a new type of dinuclear complex in which the DBT is η^1(S) coordinated to a $\{CpRu(CO)_2\}^+$ group and η^6 coordinated to $\{Cp'Ru\}^+$.

An X-ray study of $[CpRu(CO)_2(\mu_2\text{-}\eta^1(S),\eta^6\text{-DBT})RuCp^*][PF_6]_2$ (**4a**) shows that the two ruthenium moieties are on opposites sides of the planar DBT ligand. Infrared studies suggest that the Ru−S bond in the $\{CpRu(CO)_2(\eta^1(S)\text{-DBT})\}^+$ portion of **4a** is weakened by attachment of the η^6-$\{Cp^*Ru\}^+$ group to the DBT. This weakening is reflected in a much faster rate of dissociation of $[Cp^*Ru(\eta^6\text{-DBT})]^+$ than of DBT from $[CpRu(CO)_2(\eta^1(S)\text{-L})]^+$, where L = DBT or $[Cp^*Ru(\eta^6\text{-DBT})]^+$. Equilibrium studies also show that $[Cp^*Ru(\eta^6\text{-DBT})]^+$ is much less strongly coordinated than DBT to $\{CpRu(CO)_2\}^+$.

Acknowledgment. This work was supported by the U.S. Department of Energy, Office of Science, Office of Basic Energy Sciences, Chemical Sciences Division, under contract W-7405-Eng-82 with Iowa State University.

Supporting Information Available: Tables giving crystallographic data for **4a**, including atomic coordinates, bond lengths and angles, and anisotropic displacement parameters. This material is available free of charge via the Internet at http://pubs.acs.org.

OM050158Y